IEEE Open Journal of
Industry Applications

Received 7 December 2021; revised 26 April 2022; accepted 15 July 2022. Date of publication 20 July 2022;
date of current version 8 August 2022. The review of this article was arranged by Associate Editor Brant Cassimere.

Digital Object Identifier 10.1109/OJIA.2022.3192565

Minimum Energy Adaptive Load Sharing of Parallel Operated Compressors

AYMAN AL ZAWAIDEH (Member, IEEE), KHALIFA AL HOSANI (Senior Member, IEEE), IGOR BOIKO (Senior Member, IEEE), AND MOHAMMAD LUAI HAMMADIH

Electrical Engineering and Computer Science Department, Khalifa University, Abu Dhabi 127788, United Arab Emirates

CORRESPONDING AUTHOR: AYMAN AL ZAWAIDEH (e-mail: ayman.alzawaideh@hotmail.com)

This work was supported in part by Abu Dhabi National Oil Company (ADNOC), Abu Dhabi, United Arab Emirates under Grant GRC18002, and in part by Information and Communication Technology (ICT) fund, United Arab Emirates under Grant EX2019-011.

ABSTRACT Compressors operating in parallel are widely used in compressor stations on natural gas pipelines to address the required flow demands. This paper presents a design of a new control structure and a load sharing optimal adaptive controller for multiple compressors connected in parallel and equipped with variable speed drives. The load sharing optimization (LSO) controller computes the split factor to distribute the flow among the compressors which depends on the current operating conditions, with the optimization's objective being to minimize the total energy consumption. In addition, the compressor maps are continuously updated to account for any changes due to external and untraceable factors resulting in an enhancement of the LSO. The presented control structure includes a common single controller for parallel compressors, which eliminates the need for loop-decoupling. Thus, ensuring a better stability and a faster dynamics with respect to the flow or pressure process variable. The proposed control structure and the adaptive LSO performance is evaluated through simulations and a lab hardware setup. The results show an improvement of more than 4% in the total energy consumption compared to an equal load sharing scheme and more than 2.5% compared to the equal distance to surge industrial scheme. This efficiency improvement leads to significant energy cost saving over large periods of time.

INDEX TERMS Adaptive control, compressors, gas industry, industry application, optimization of compressor operation.

I. INTRODUCTION

Gas compressors are used in various industrial applications such as in gas storage, gas transportation via pipelines, air separation plants, and for compressed air production [1]. Gas compressors consume a significant amount of energy [2], with a notable economical impact on industrial operators. Therefore, research aimed at increasing the operational efficiency of compressors is of high importance [3], [4]. Gas compressors used in industrial applications are often configured in either parallel or series interconnections. The series configuration is normally used to increase the compression ratio, while the parallel configuration is needed to raise the flow [5].

Typically, the dispatch center sends the set-point (flow or pressure) to the compressor station, which in turn provides the speed set-points to the individual compressors through a load sharing controller. This is done in accordance with the operational limits of the individual compressors to operate them at an equal distance to the surge point [4]. However, while maintaining an equal distance to surge provides a certain stability margin, it does not take into account the individual compressor efficiencies, which results in a sub-optimal operation in terms of total energy consumption.

The major development in the field of compressor stations on natural gas pipeline has been the shift from fixed speed drivers, in which the control was performed on defining the active compressors and regulating the amount of compressed gas circulating and throttling, towards compressor units being driven by electric variable frequency drives (VFDs) and variable-speed gas turbines [4], [6]. This shift ensured a wider range of compressor operation and resulted in an improvement of the overall system efficiency, achieved through the separate control of each individual compressor. However, the structural

complexity of compression networks having units connected in both series and parallel necessitates in solving the problem of load sharing through what is often referred to as compressor Load Sharing Optimization (LSO) [3], [4], [7], [8].

The LSO goes beyond basic load sharing; it considers the individual compressor performance maps to optimize the number of active compressors [3], and to provide individual speed set-points to the drives to achieve a certain criterion such as minimizing the total energy consumption [4], [8]. The main challenge faced in the LSO is that it highly depends on the accuracy of the compressor and performance maps which tend to vary due to external and untraceable factors such as erosion and fouling [7], [9]. A typical update of the maps is carried out every 10 to 20 years, or when there is a major shutdown, or a major failure of the compression train. The infrequent update of the performance maps leads to the deterioration of the LSO advantages [10].

Various research examples of LSO are found in recent literature. A recursive update of the compressors maps followed by an online optimization is presented in [11]. In [12] various factors influencing the economic potential and cost of compressor stations are studied. A surrogate model for a centrifugal compressor is proposed using a moving least squares algorithm in [13]. [14] and [15] carry out a multi-objective optimization to maximize throughput of the station and to minimize the total energy consumed, where the findings were presented as several Pareto fronts. [16] solved a nonlinear programming problem based on a detailed mathematical derivation of a compression network. The objective function was the minimum of the total energy consumption and was achieved through varying the speed set-points of the compressors. The uncertainty of the compressors maps are currently addressed by the industry through the two-step approach [3], [4], [8], in which the compressors maps are initially updated using a static nonlinear regression approach, followed by running the LSO. [3] proposed an optimization methodology for compressors operating in parallel that combines a real-time LSO and compressor scheduling. The presented optimization algorithm was verified on an industrial case study. Publication [17] developed a load sharing strategy based on a degradation indicator that reflects the extent of fouling of compressor blades and the roughening of its surfaces. The proposed load sharing managed to slow down degradation by reducing the need for the degraded compressor while increasing the set-points for the healthy compressor. Mitigating the degradation was accomplished by decreasing the torque applied to the compressor. [18] investigated the application of Modifier adaptation (MA) for the load sharing optimization of series-connected compressors. The MA uses online measurements to approximate plant gradients which are then used to update the proposed model. This work was extended in [1] by allowing the compressor to be operated close to the surge line for the solution of the LSO problem. [19] proposed a model that incorporates the effect of compressor degradation caused by fouling on the total power consumption and analyzed its influence on the LSO problem. The relationship between centralized MA and proximal gradient is investigated in [20]. The developed MA scheme uses plant gradient in both the interconnection variables and the decision variables, and it ensures confidentiality of the local plant data and models. The proposed algorithm was then tested for LSO on series-connected compressors. In publication [21], an algorithm for the control of a few compressors is presented, in which the problem is solved through mixed integer nonlinear programming.

Many publications focus on the design of compressor controller and performance enhancement. An application of a linearized model predictive control (MPC) to regulate the process through the driver's torque and to control the anti-surge recycle valve opening is proposed in [22]. In [23], a multivariable control system is developed for a class of centrifugal compressors. A linear quadratic Gaussian control with integral action and a MPC are applied to control the inlet guide vane and the rotational speed. This work was extended to include the anti-surge control problem in [24]. Publication [25] proposed a procedure for compressor system identification and an application of an adaptive gain scheduling PI controller to regulate the required mass flow rate. In [26], a fuzzy logic controller is applied to a constant speed compressor for surge suppression.

The recognized state-of-the-art control strategies for load-sharing used in the industry are those proposed by Compressor Controls Corporation (CCC), Dresser Rand, and General Electric (GE). The load sharing scheme in these control strategies is based on the principle of equal distance to the surge line [27]–[29]. Publication [29] provides a control system design which specifies the required export flow of individual compressors such that an equal load balance is ensured. Publication [30] presents a control method for multiple turbo-compressors, each driven by a separate controller, where the main objective is to maintain the operating point at a specific surge line. [31] describes a control system and a design for controlling several compressors to provide efficient load sharing between the compressors. One compressor is assigned as the lead compressor, and it supplies its operating parameters to all other lag compressors. Compressors are gradually added to or shed form the load subject to certain time delays.

In summary, the load sharing scheme shared by the industry leaders implemented in various oil and gas fields deals with operating parallel compressors at an equal distance to surge, which results in a sub-optimal energy consumption. Another important note is that their control structure have multiple separate PID controllers for each compressor, which requires a loop-decoupling between the compressor trains. This entails a slower dynamic response to set point changes or disturbances. While the recent works cited above report improved efficiency of the compressor station, the optimization LSO algorithms are of high computational complexity, and ensuring global minimum is a challenging task [8], [11]. Furthermore, the recent publications tend to lack the verification of their designed LSO algorithm on an experimental setup [4], [8], [11], [16], [32].

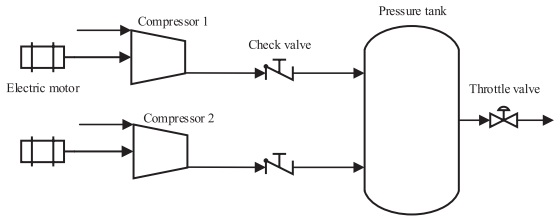

FIGURE 1. Parallel compression system schematic.

The present paper discusses a single load sharing optimal adaptive controller for multiple compressors connected in parallel in a compressor station. Unlike previous works, the proposed approach eliminates the need for having a separate controller for each compressor in compressor train. The feedback control loop and the adaption control loop in the proposed system are decoupled, hence, achieving a better dynamic performance. In addition, the stability of the pressure/flow controller is easier to ensure compared to having multiple process controllers. Besides, the proposed method uses an exponential recursive least squares algorithm to account for the changes in the performance maps used in the online optimization algorithm. Finally, the proposed algorithm results in an optimal energy consumption compared to an equal load sharing scheme and compared to the popular industrial scheme of equal distance to the surge [27]–[29], as verified by simulations and hardware implementation.

This paper is organized as follows. Section II presents the parallel compression system mathematical model, compressor performance maps, and the map adaptation based on the exponential least square algorithm. The optimal adaptive load sharing algorithm is discussed in Section III. Section IV describes the overall designed control system structure, and its stability analysis is derived in Section V. In Sections VI and VII, the proposed system structure and the optimization algorithm are tested through simulations and a hardware prototype. Finally, a summary and a conclusion are provided in Section VIII.

II. COMPRESSION SYSTEM

The gas network delivery requirements in terms of the desired flow and discharge pressure can be attained through the use of multiple compressors in series and/or parallel. A series connection is usually set to increase the overall required discharge pressure, whereas a parallel connection is used to meet the high flow demand. The latter topology is the main focus of this paper, and will be discussed in detail.

A general schematic of parallel operated compression system is depicted in Fig. 1. We consider two parallel compressors coupled with a common plenum and a throttle/discharge valve. The compressor discharges air flow through a duct of an area A and a length L, before entering a common plenum (pressure tank). The duct is connected to a check valve to prevent the reverse air flow during transients of pressure change of both of the compressors. In this paper, the upstream (suction side of both of the compressors) and the downstream (after the discharge valve) are considered to be at the ambient atmospheric condition for the simulations and the hardware implementation prototype.

In this paper, we consider the situation of the small common receiver volume (tank) being available, which is the case of booster and transfer compressors connected to a common pipe. In such case we can consider that the outflow rate from this common receiver is equal to the sum of the flow rates of all the compressors.

A. MATHEMATICAL MODEL

Modeling of compression systems have been historically investigated through a non-dimensional model [33], which was used mainly to simulate both surge and rotating stall. It is suitable to be utilized under the assumption of a constant speed of rotation [34]. In the present paper, the compressor rotational speed is considered variable and treated as a state, like in publications [22], [34]–[37]. The mathematical representation of the compression system dynamics is based on the mass balance of gas in the plenum, momentum balance of gas in the duct, the rotating shaft dynamics, and the relaxation equation describing the compressor transition from one steady state to another, which are presented as follows [38], [39]:

$$\frac{dp}{dt} = \frac{a_{01}^2}{V}(w - w_{out}) \tag{1}$$

$$\frac{dw}{dt} = \frac{A}{L}(\Psi_c p_{01} - p) \tag{2}$$

$$\frac{d\Psi_c}{dt} = \frac{1}{\tilde{\tau}}(\Psi_{c,ss} - \Psi_c) \tag{3}$$

$$\frac{d\omega}{dt} = \frac{1}{J}(\tau_d - \tau_c) \tag{4}$$

where p is the tank pressure (Pascal), w is the mass flow rate through the duct (kg/s), Ψ_c is the compressor pressure rise, τ_d is the driver torque, τ_c is the compressor torque, $a_{01} = \sqrt{\kappa R_{sp} T}$ is the sonic velocity at ambient conditions, V is the volume of the plenum, A is the cross-sectional area of the duct and L is its length, J is the inertia of the overall driver compressor system, $\Psi_{c,ss}$ is a (nonlinear) steady-state compressor pressure rise characteristic, and $\tilde{\tau}$ is the compressor time constant.

The temperature of the gas tends to increase as a result of the compression process. The equation of the compressor discharge temperature is [40]:

$$T_{out} = T_{in}\left(\frac{p_{out}}{p_{in}}\right)^{\frac{\kappa-1}{\kappa\eta_p}} \tag{5}$$

where κ is the specific heat ratio and η_p is the polytropic efficiency.

The mass air flow through the throttle valve is given by the (St. Venant and Wantzel formula [41]):

$$G_v = A_t c_d p_1 \sqrt{\frac{\gamma}{R_{sp}T_1}\left(\frac{2}{\gamma+1}\right)^{\frac{\gamma+1}{\gamma-1}}} \Psi\left(\frac{p_2}{p_1}\right) \tag{6}$$

where A_t is the smallest cross-sectional area of the flowing element, c_d is the discharge coefficient (such that $A_t c_d$ is the effective cross-sectional area of the valve opening), R_{sp} is the specific gas constant for air, T_1 is the input temperature, γ is the isentropic coefficient ($\gamma = 1.4$ for air), and $\Psi(\frac{p_2}{p_1})$ is the flow function given by:

$$\Psi\left(\frac{p_2}{p_1}\right) = \begin{cases} 1 \quad if \quad \frac{p_2}{p_1} \leq \beta_c \\ \sqrt{\frac{2}{\gamma-1}\left(\frac{\gamma+1}{2}\right)^{\frac{\gamma+1}{\gamma-1}}}\sqrt{\left(\frac{p_2}{p_1}\right)^{\frac{2}{\gamma}} - \left(\frac{p_2}{p_1}\right)^{\frac{\gamma+1}{\gamma}}} \quad if \quad \frac{p_2}{p_1} \geq \beta_c \end{cases}$$

where $\beta_c = (\frac{2}{\gamma+1})^{\frac{\gamma}{\gamma-1}}$ is the critical pressure ratio ($\beta_c = 0.528$ for air).

The valve characteristics may be represented by a polynomial approximation such as:

$$w_{out}(V_{op}, P_2) = a_1(V_{op})P_2^2 + a_2(V_{op})P_2 + a_3(V_{op}) \tag{7}$$

where V_{op} is the percentage of the valve opening and a_i is a polynomial calculated based on the valve opening as given below.

$$a_i(V_{op}) = c_{i1}V_{op}^3 + c_{i2}V_{op}^2 + c_{i3}V_{op} + c_{i4}$$

The parameters c_{ii} may be determined using the Matlab function *polyfit*.

B. COMPRESSOR PERFORMANCE MAPS

The compressor discharge pressure or pressure ratio (Ψ_c) is determined mainly based on the rotational speed of the rotor and the mass or the volumetric flow rate through the compressor. The dynamics of Ψ_c can be expressed mathematically as a function of the detailed boundary conditions of inlet and outlet of the compressors [38], [39], [42]. This adds a high complexity to the overall system. Another approach which is commonly used is through the representation of the compressors performance maps by polynomial approximation [25], [39], [43]. In this paper, the experimental data are approximated by polynomials, where the coefficients are found through the solution of the linear regression problem via least squares.

Let us define the compressor characteristics as:

$$y(\boldsymbol{\alpha}, w, N) = \alpha_1 + \alpha_2 w + \alpha_3 N + \alpha_4 N w + \alpha_5 w^2 + \alpha_6 N^2 \tag{8}$$

where y can be the compressor discharge pressure, efficiency, or electric power consumption, w is the mass flow rate (kg/hr), and N is the compressors rotational speed (rpm). Usually measurements of flow rate, pressure, rotational speed and electric energy are available in compressor control systems, so that the proposed approach involving updates of the compressor maps and performance maps does not require additional instrumentation. It should be noted that the approximations (8) are linear in the parameters α_i. Using least squares algorithm, the minimum is obtained at [44]:

$$\hat{\boldsymbol{\theta}} = \boldsymbol{\theta} = (\boldsymbol{\Phi}^T\boldsymbol{\Phi})^{-1}\boldsymbol{\Phi}^T\mathbf{Y} \tag{9}$$

where $\mathbf{Y}$ is the observed vector variable, $\boldsymbol{\Phi}^T$ is a vector of known functions (regressors vector), and $\hat{\theta}$ is the parameters vector to be determined given by:

$$\hat{\boldsymbol{\theta}} = \begin{bmatrix} \alpha_1 & \alpha_2 & \alpha_3 & \alpha_4 & \alpha_5 & \alpha_6 \end{bmatrix}^T$$

It is worth noting that the matrix $\boldsymbol{\Phi}^T\boldsymbol{\Phi}$ is positive definite. This is due to the matrix $\boldsymbol{\Phi}$ having a full rank column ($r = 6$), which results in $\boldsymbol{\Phi}^T\boldsymbol{\Phi}$ being invertible.

C. LEAST SQUARES AND REGRESSION MODEL

The optimization algorithm uses fitted approximations of the compressor maps and performance maps. Variations in gas properties, equipment damage, disturbances, decreased lifetime of the equipment or fouling can lead to inaccuracies in these approximations. This problem can be circumvented using each compressor's available measurements for online-parameter estimation. Without online adaptation, the optimization algorithm would lead to steady-state errors which would have to be adjusted by the process controller in a non-optimal way.

In adaptive controllers the observations are obtained sequentially in real time. To save computation time, it is desirable to make the computations recursively. Computation of the least squares estimate ($\hat{\theta}$) can be organized in a recursive way, so that the results for time t can be obtained from the estimates at time $t-1$ as a certain increment to the latter. Additionally, introduction of forgetting can give higher weights to the recent measurements versus older ones. The recursive least squares estimate with exponential forgetting (ERLSE) can be written as [45]:

$$\hat{\boldsymbol{\theta}} = \hat{\boldsymbol{\theta}}(t-1) + \mathbf{K}(t)\left(y(t) - \phi^T(t)\hat{\theta}(t-1)\right) \tag{10}$$

where the matrices $\mathbf{K}(t)$ and $\mathbf{P}(t)$ can be computed as:

$$\mathbf{K}(t) = \mathbf{P}(t)\phi(t) = \mathbf{P}(t-1)\phi(t)\left(\lambda_F + \phi^T(t)\mathbf{P}(t-1)\phi(t)\right)^{-1}$$

$$\mathbf{P}(t) = \left(\mathbf{I} - \mathbf{K}(t)\phi^T(t)\right)\mathbf{P}(t-1)/\lambda_F$$

where λ_F is the forgetting factor. The exponential recursive least square algorithm [45] can be used when the system parameters are changing continuously but slowly. The forgetting factor ($0 \leq \lambda_F \leq 1$) introduces a time varying weight to the performance maps data. The new data will have a higher weight compared to the old data used for the polynomial approximation, which insures a faster convergence of the parameters vector ($\hat{\theta}$) in (9).

In the present work, the steady state operating conditions are continuously recorded. If the difference between the power performance maps and the current reading, or the discharge pressure difference between the compressor map and the pressure sensors value is considerably high, the operating conditions are recorded. The ERLSE algorithm runs after recording a number of points to have a better approximation of the compressor and performance maps.

III. OPTIMAL ADAPTIVE LOAD SHARING ALGORITHM

The load sharing problem is challenging, as it largely depends on finding the optimum operating point based on

the efficiency/energy performance maps of the compressors. Load sharing implies setting the optimal relation between flows, speeds and discharge pressure to maximize the total efficiency, while satisfying the varying gas demand of the parallel-operated compressors, which results in saving much energy [4], [11], [32]. In this paper, the designed optimization algorithm's main objective is to provide an on-line adaptation of the load split factor based on solving the load sharing problem at current operating conditions. The proposed structure of the adaptive control system allows us to formulate the optimization problem as having the number of decision variables being one less than the number of compressors. For the load split factor between the two compressors, it is only one decision variable. Algorithms of one-dimensional optimization can guarantee finding the true minimum on an interval. The optimization decision variable is set to be the load split factor of the parallel operated compressors (λ). The variation of λ would allow one to minimize the total energy consumption through operating the compressors at a different load split factor. The compressors load split factor is defined as:

$$\lambda = \frac{\bar{N}_1}{\bar{N}_1 + \bar{N}_2} \tag{11}$$

where $\bar{N}_i = \frac{N_i}{N_{imax}}$, given that N_i, and N_{imax} are the speed and the maximum speed of the ith compressor, respectively.

Fig. 2 shows a flowchart of the optimization algorithm. The algorithm runs after the plant reaches a steady state in terms of the pressure or total mass flow. Then the controller output, compressors suction pressure and temperature, total mass flow, and the required pressure set point are recorded. Based on the compressor and performance maps of both of the compressors and the limitation of the surge lines, a range of acceptable λ is calculated to act as a constraint/limitation. The range of the load split factor depends on the compressors maximum and the minimum rotational speeds, surge limitations, and the required discharge pressure. The minimum load split factor ($\lambda_{\min}$) can be calculated by finding the minimum allowable flow before going to surge of the first compressor and then solving for the speed that corresponds to that flow at the specified pressure set point. Then the flow through the second compressor is calculated such that the total flow is maintained, followed by finding the speed that corresponds to the specified flow and pressure set point. The maximum load split factor ($\lambda_{\max}$) can be found similar to ($\lambda_{\min}$), by initially finding the minimum allowable flow trough the second compressor before going to surge. $\lambda_{\min}$ and $\lambda_{\max}$ are calculated mainly from the compressor maps (8) and (11). The range of acceptable λ (load split factor) ensures that when the first compressor is more loaded compared to the second one, the second compressor does not go into surge, and vice versa. Then by varying λ, the compressors speeds and their corresponding mass flows are calculated. Furthermore, from the compressors performance maps, their energy consumption or efficiencies can be evaluated, and finally the cost function of the total energy or efficiency is recorded for the respective

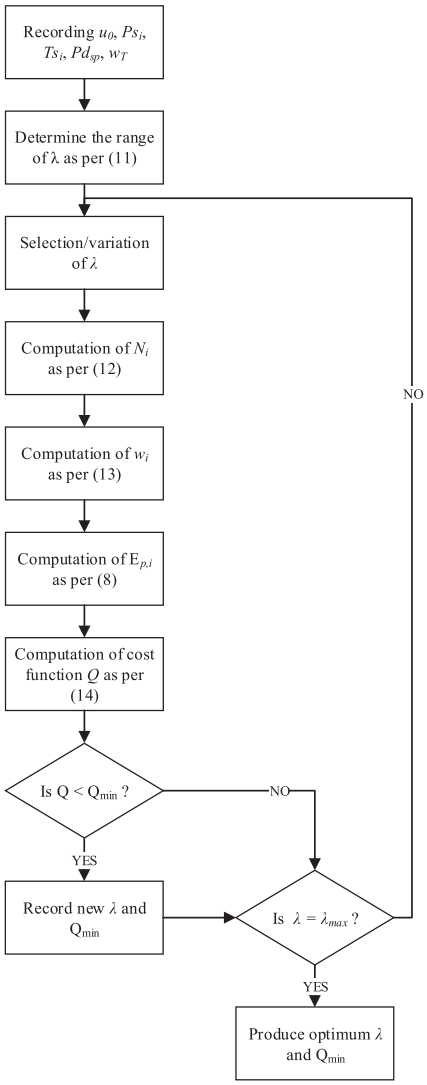

FIGURE 2. Optimization algorithm logic diagram.

λ. The procedure is repeated for the range of the acceptable λ, and the minimum cost function is produced. The optimization algorithm is executed on a periodic basis (every 50 s in the implementation considered below) to adjust the load split factor λ depending on the variations of the current system.

The LSO problem for a system consisting of multiple parallel compressors is typically expressed as:

$$\begin{aligned} &minimize \quad E_{P_T} = \sum_{i=1}^{k} E_{P_i} \\ &subject\ to \quad P_{d_i} = P_{d_{sp}}\ or\ w_{T_{sp}} = \sum_{i=1}^{k} w_i, \\ &\qquad\qquad N_i \le N_{i_{\max}}\ and\ \lambda_{\min} \le \lambda \le \lambda_{\max} \end{aligned}$$

where E_{P_i} is the electric power consumption of the ith compressor which is based on the experimental performance maps

expressed in (8). The ranges of $\lambda_{\min}$ and $\lambda_{\max}$ (11) are determined based on the surge lines of the compressor maps parallel compressors. This ensures that the minimum and the maximum load sharing/split between the compressors would not drive the compressor with the lower load towards surge. The current operating control signal is recorded, which allows one to compute the speeds of the compressors by:

$$N_1 = 2{\cdot}u{\cdot}\lambda{\cdot}N_{1_{\max}}$$
$$N_2 = 2{\cdot}u{\cdot}(1-\lambda){\cdot}N_{2_{\max}} \tag{12}$$

The flow can then be computed from (8) as:

$$w_i = \frac{-(\alpha_2+\alpha_4 N_i)}{2\alpha_5} - \frac{\sqrt{(\alpha_2+\alpha_4 N_i)^2 - 4\alpha_5(\alpha_1+\alpha_3 N_i+\alpha_6 N_i^2 - P_{d_{sp}})}}{2\alpha_5} \tag{13}$$

Finally, the total energy consumption is computed as the following sum of parallel operated compressors:

$$Q = E_{P_T} = \sum_{i=1}^{k} E_{P_i} \tag{14}$$

where E_{P_i} is based on the polynomial approximation (8) of the performance map. These steps are repeated for the determined range of acceptable λ's, and the load split factor (λ) that corresponds to the minimum energy consumption is recorded. It should be noted that if the parallel compressors are identical, the solution of the load sharing problem (LSO) will be trivial, meaning that all of the compressors will be operated at an equal loading rate. However, if the compressors do not have identical characteristics (compressor maps and performance maps), then a LSO problem needs to be solved to load each compressor at a rate that results in the optimum energy consumption.

IV. DESIGNED SYSTEM CONFIGURATION AND CONTROLLER

The proposed control structure involves two loops as depicted in Fig. 3, a feedback control loop and an adaptive control loop. Unlike the current practice where there are multiple PID controllers for each compressor and a loop-decoupling controller between them, the proposed control structure has a single PID controller for multiple parallel compressors which ensures faster loop dynamics to the change in the set-point or applied disturbances. It should be noted that the adaptation loop is slow in comparison to the process loop, such that a quasi-static approach can be used and the dynamics of the adaptation and the dynamics of the process are decoupled. We shall assume that in the adaptation loop, which is executed in discrete time, the process transients have settled to the respective steady states within the time discrete (which is selected 50 s in the considered example and experiment). Analysis of the stability of the process loop, a constant value of the load split factor may be assumed (because it is not changed within the time discrete of the adaptation loop). The developed structure has a slow changing parameter λ provided by the adaptive loop. This design leads to approximately constant process gain at different values of λ, so that increase of flow due to the speed increase of one compressor will be compensated for by the equal decrease of flow due to the decrease of speed of the other compressor. At the same time the adaptive and the process feedback loops are decoupled.

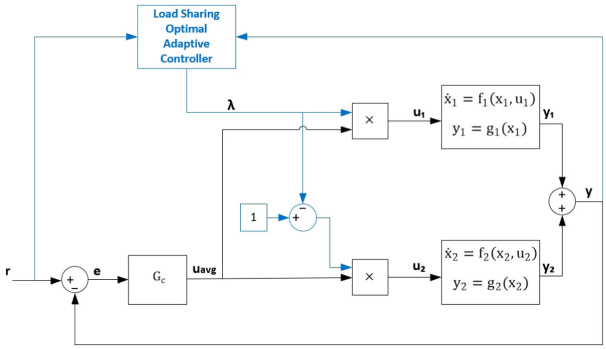

FIGURE 3. The control system structure for a nonlinear compressor network model of two parallel compressors.

The control system structure of the compression network process depicted in Fig. 3 comprises one common PID process controller to regulate the total discharge flow y measured by a flow transmitter or discharge pressure measured by a pressure transmitter and a common load-sharing optimal adaptive controller. Compressor stations on natural gas pipelines are typically composed of multiple parallel compressors as presented in Fig. 3 for operational flexibility. Dynamics of each compressor can be modeled given by a set of nonlinear differential equations:

$$\dot{x}_1 = f_1(x_1, u_1)$$
$$y_1 = g_1(x_1)$$

where x_1 is a state vector of first compressor, u_1 is an input scalar given as speed demand for first compressor, f_1 and g_1 are nonlinear functions, and y_1 is an output of the first compressor (for example flow). The output signal (y_1) being the mass flow or the discharge pressure and the dynamics of the compressor ($\dot{x}_1$) are determined by the set of formulas (1)–(8).

The adaptive LSO algorithm runs every 50 s and computes a load split factor (λ), which is used to split the PID controller's output into individual speed commands for each of the parallel VFDs; for two compressors, the individual speed commands are obtained through multiplication of the PID output with λ and $1-\lambda$. As long as the operating conditions do not change, the load split factor remains constant. Variable load split factor (λ) is an important feature of our control structure, which allows us to load one compressor more compared to the other one without altering feedback loop dynamics. Variation of the

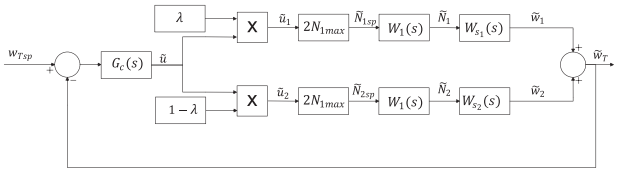

FIGURE 4. Block diagram of the designed control structure.

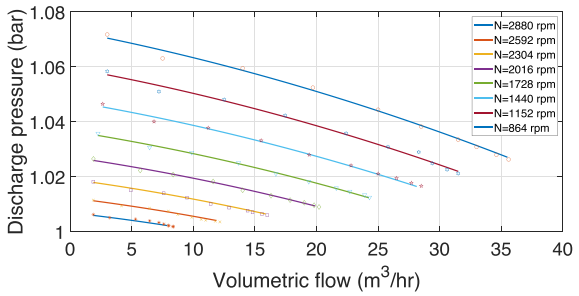

FIGURE 5. Compressor discharge pressure (bar) vs. Volumetric flow (m^3/hr) polynomial fit.

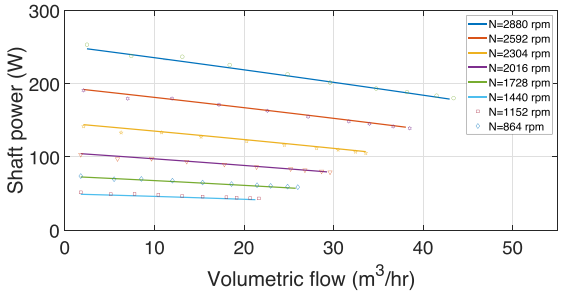

FIGURE 6. Compressor shaft power (W) vs. Volumetric flow (m^3/hr) polynomial fit.

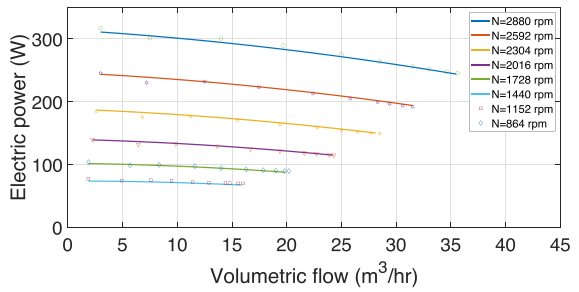

FIGURE 7. Compressor Electric power (W) vs. Volumetric flow (m^3/hr) polynomial fit.

load split factor is aimed at minimizing the overall consumed energy.

V. STABILITY ANALYSIS

The block diagram of the parallel operated compressors is depicted in Fig. 4 where each $W_i(s)$ represents the combined transfer function of the induction motor and its VFD. These dynamics are approximated by a first order plus dead time

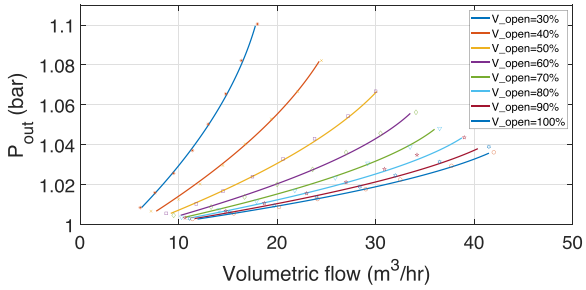

FIGURE 8. Throttle valve input pressure (bar) vs. Volumetric flow (m^3/hr) polynomial fit.

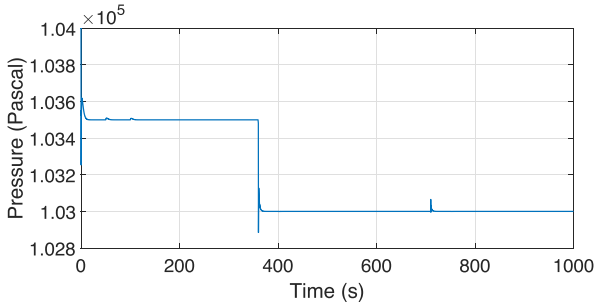

FIGURE 9. Plenum pressure (Pascal), Step changes in pressure set-point and valve opening at 360 s and 710 s, respectively.

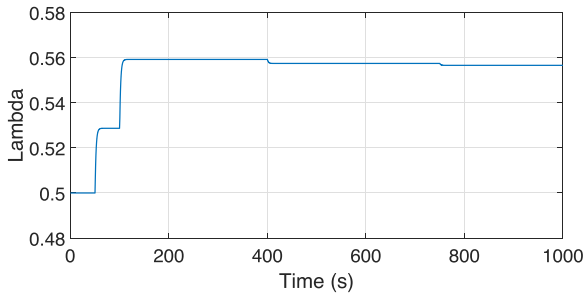

FIGURE 10. Compressor's load split factor (λ) reaction to pressure set point and load changes.

model.

$$W_i(s) = \frac{e^{-\tau_i s}}{T_i s + 1} = \frac{N_i}{N_{isp}} \tag{15}$$

where T_i and τ_i are the time constant and the dead time that are determined based on the hardware set-up.

Rewriting (1)–(3) in a state space representation yields:

$$\begin{aligned}
\dot{x}_1 &= \frac{a_{01}^2}{V}\left(x_2 - k_1\left(a_1 x_1^2 + a_2 x_1 + a_3\right)\right) \\
\dot{x}_2 &= \frac{A}{L}(x_3 - x_1) \\
\dot{x}_3 &= \frac{1}{\tilde{\tau}}\left(k_2(\alpha_1 + \alpha_2 x_2 + \alpha_3 u + \alpha_4 x_2 u + \alpha_5 x_2^2 + \alpha_6 u^2) - x_3\right)
\end{aligned} \tag{16}$$

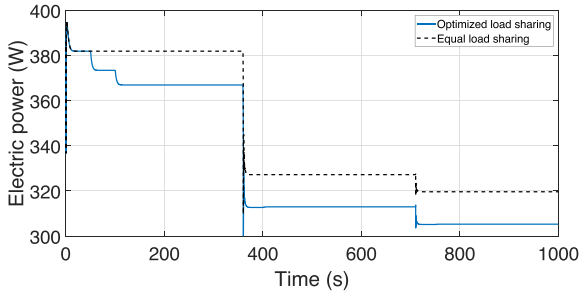

FIGURE 11. Compressors total electric power consumption (W) at an equal and an optimal load sharing.

where x_1 is the tank pressure (p), x_2 is the flow through the compressor (w), x_3 is the compressor discharge pressure (p_d), $k_1 = 10^5$ and $k_2 = 1/3600$ are constants to transform the flow and pressure units to kg/s and $Pascal$.

Linearization of (16) around the equilibrium point, where the superscript ($\tilde{x}_i$) is the perturbation/increment of the respective variables with respect to a value at the corresponding equilibrium point, yields the following:

$$\begin{aligned}\dot{\tilde{x}}_1 &= A_1\tilde{x}_2 + A_2\tilde{x}_1\\ \dot{\tilde{x}}_2 &= -A_3\tilde{x}_1 + A_3\tilde{x}_3\\ \dot{\tilde{x}}_3 &= A_4\tilde{x}_2 + A_5\tilde{x}_3 + B_1\tilde{u}\end{aligned} \tag{17}$$

where

$$\begin{aligned}A_1 &= \frac{a_{01}^2}{V}k_1\left(a_2 + 2a_1x_1^*\right)\\ A_2 &= \frac{a_{01}^2}{V}\\ A_3 &= \frac{A}{L}\\ A_4 &= \frac{1}{\tilde{\tau}}k_2\left(\alpha_2 + \alpha_4u^* + 2\alpha_5x_2^*\right)\\ A_5 &= -\frac{1}{\tilde{\tau}}\\ B_1 &= \frac{1}{\tilde{\tau}}k_2\left(\alpha_3 + \alpha_4x_2^* + 2\alpha_6u^*\right)\end{aligned}$$

where x_i^* and u^* are the steady state values of the states and the compressor speed, respectively. The transfer function from the compressor speed perturbation to its flow perturbation can be represented as follows:

$$W_{ci}(s) = \frac{A_3B_1(s - A_1)}{s^3 - (A_1 + A_5)s^2 + (A_1A_5 + A_2A_3 - A_3A_4)s + A_3(A_1A_4 - A_2A_5)} = \frac{\tilde{w}_i}{\tilde{N}_i} \tag{18}$$

Let the compressor transfer function be defined as:

$$\begin{aligned}W_{s1}(s) &= \frac{\tilde{w}_1}{\tilde{u}}\\ &= 2\cdot\lambda\cdot N_{1_{\max}}\cdot W_1(s)\cdot W_{c1}(s)\\ W_{s2}(s) &= \frac{\tilde{w}_2}{\tilde{u}}\\ &= 2\cdot(1-\lambda)\cdot N_{2_{\max}}\cdot W_2(s)\cdot W_{c2}(s)\end{aligned} \tag{19}$$

The overall closed loop system can be computed as:

$$W_{cl}(s) = \frac{G_c(s)W_{pl}(s)}{1 + G_c(s)W_{pl}(s)} \tag{20}$$

where

$$\begin{aligned}W_{pl}(s) &= W_{s1}(s) + W_{s2}(s)\\ G_c(s) &= k_p\left(1 + \frac{1}{T_is}\right)\end{aligned}$$

Checking the eigenvalues ($Re(\lambda_i) < 0$) of the 9th order closed loop system (20) ensures stability of the designed control system. All eigenvalues of the closed loop system (20) have a negative real parts for the designed PI parameters at multiple operating conditions (defined by different pressure set-points and outlet valve openings, which represents different loads).

VI. SIMULATIONS

The performance verification of the proposed control structure and the on-line load sharing algorithm is first done via Matlab/Simulink simulations. The generated compressor performance maps are represented by a polynomial curve fitting function (8). The compressor discharge pressure (Pascal), shaft power (W), and electric power consumption (W) vs. volumetric flow rate (m^3/hr) at a range of operating speeds (rpm) are shown in Figs. 5, 6, and 7, respectively. The dynamics of the throttle valve (load) was experimentally extrapolated and approximated as a polynomial function at different valve openings as depicted in Fig. 8. The compressors and performance maps and the load characteristic are based on the experimental setup prototype which is discussed in the next section. Table 1 shows the parameters of the parallel compressors system, and Table 2 provides the polynomial coefficients of the first compressor based on (8) & (9).

The compression system depicted in Fig. 1 is developed in Matlab/Simulink based on (1)–(4) and on the derived compressor maps polynomial approximations (8). The throttle valve (load) is opened at 80%, and the initial load split factor (λ) is set to be 0.5 (equal load sharing between the two compressors). The optimization algorithm runs every 50 s which depends mainly on the current control value, suction pressures and temperatures of the parallel compressors, their electric power consumption performance maps, and the required pressure at the plenum.

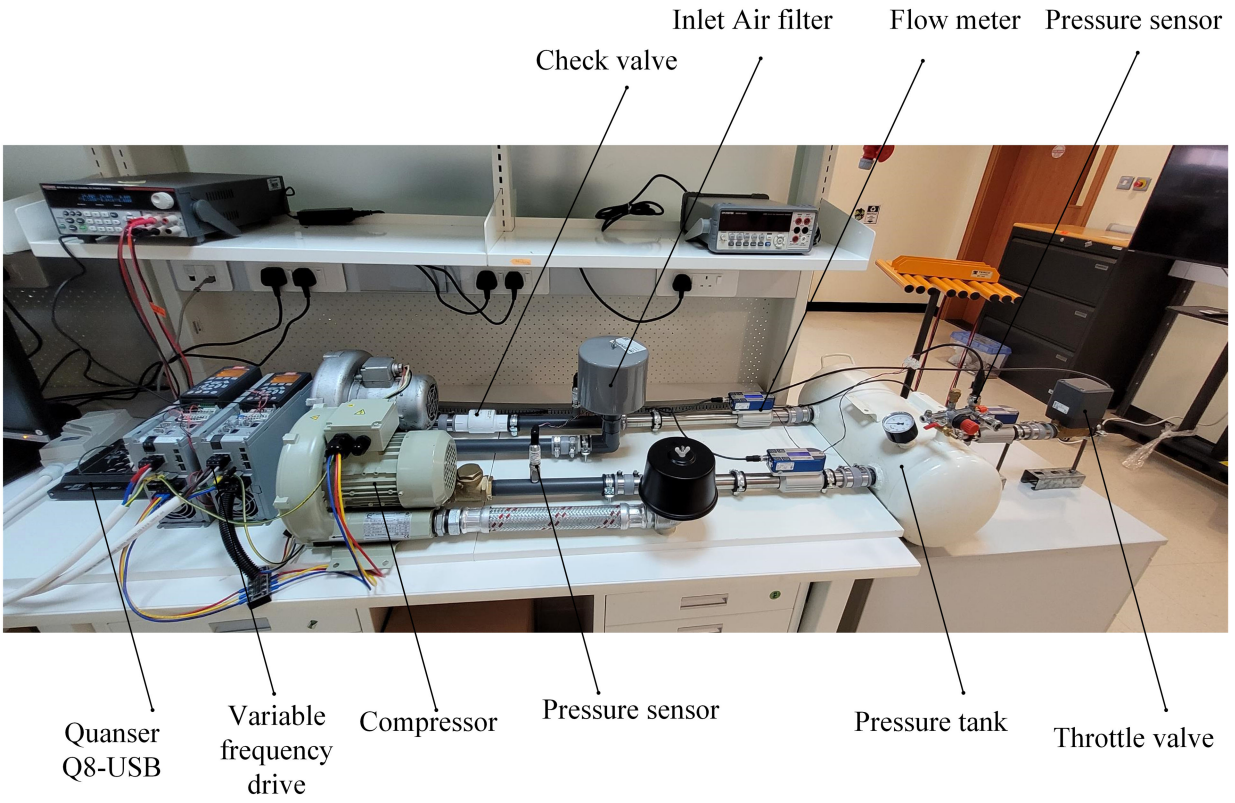

FIGURE 12. Parallel compression system experimental setup.

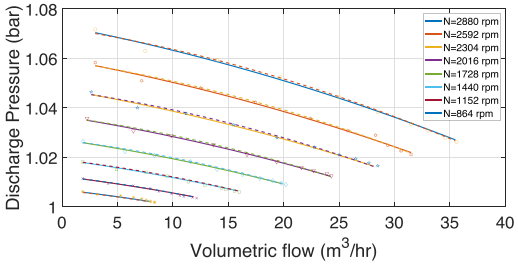

(a) Discharge pressure map of the first compressor before (solid lines) and after (dashed lines) map adaptation using ERLSE

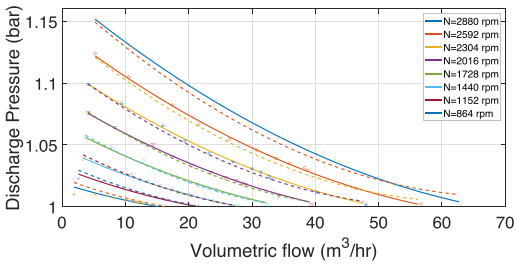

(b) Discharge pressure map of the second compressor before (solid lines) and after (dashed lines) map adaptation using ERLSE

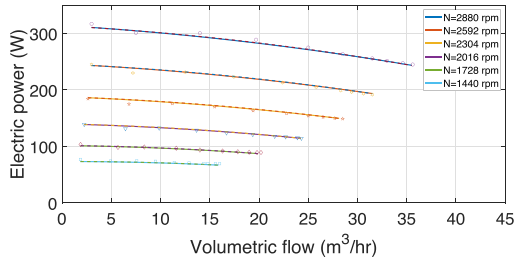

(c) Electric power performance map of the first compressor before (solid lines) and after (dashed lines) map adaptation using ERLSE

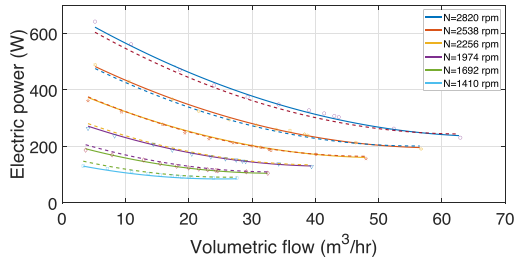

(d) Electric power performance map of the second compressor before (solid lines) and after (dashed lines) map adaptation using ERLSE

FIGURE 13. Compressors 1 and 2 map adaptation.

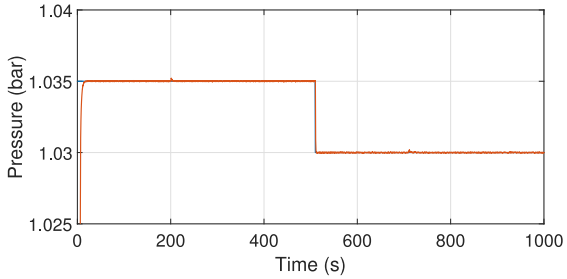

(a) Plenum pressure response to step changes in pressure set-point and valve opening at 510s and 710s, respectively (experiment)

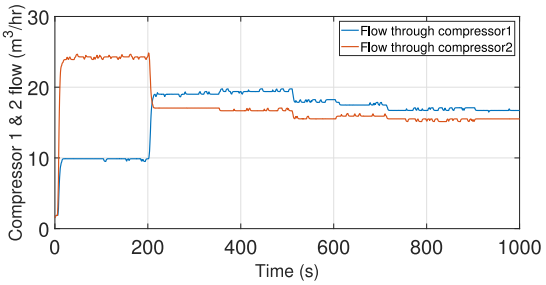

(b) First and second compressor volumetric flow rate (experiment)

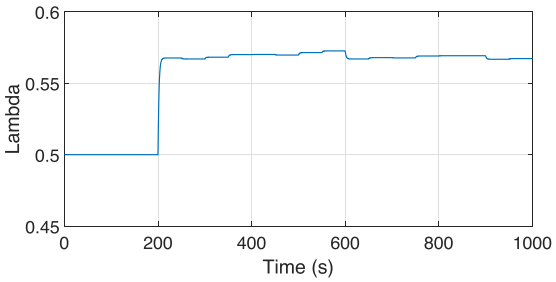

(c) Load split factor (λ) reaction to changes of pressure set-point and valve opening (experiment)

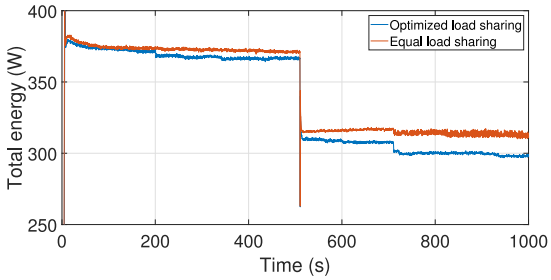

(d) Total energy consumption at equal and optimal load sharing (experiment)

FIGURE 14. Parallel compressor system energy consumption and dynamics response to changes in pressure set-point at 510 s (1.035 bar to 1.030 bar) and valve opening at 710 s (80% to 70%).

TABLE 1. Parameters of the Parallel Compressors System

Description	Parameter	Nominal Value
Compressor Inlet pressure	P_{01} [bar]	1.0
Compressor time constant	$\tilde{\tau}$ [s]	0.50
Duct cross-sectional area	A [cm^2]	4.64
Duct length	L [m]	1.50
Specific heat ratio	κ	1.40
Valve outlet pressure	P_2 [bar]	1.0
Valve effective cross-sectional area	$A_t c_d$ [cm^2]	4.30
Specific gas constant for air	R_{sp} [$\frac{N \cdot m}{mol \cdot K}$]	286.9
Isentropic coefficient for air	γ	1.40
Forgetting factor	λ_F	0.9
Compressor 1 maximum speed	N_{1max} [rpm]	2880
Compressor 2 maximum speed	N_{2max} [rpm]	2820
Moment of inertia	J [$kg \cdot m^2$]	0.005297
Motor dynamics time constant	T_i [s]	0.081
Motor dynamics dead time	τ_i [s]	0.01

TABLE 2. Polynomial Functions Coefficients (8) for the compressor1

Parameters vector $\hat{\theta}$	Discharge pressure[bar]	Electric power[W]	Shaft power[W]
α_1	0.9986	80.115	51.485
α_2	-3.429×10^{-4}	1.0815	0.937
α_3	2.431×10^{-6}	-0.0907	-0.0723
α_4	-1.793×10^{-7}	-7.422×10^{-4}	-8.739×10^{-4}
α_5	-1.234×10^{-5}	-0.0262	-0.0025
α_6	8.128×10^{-9}	5.969×10^{-5}	4.919×10^{-5}

The initial required plenum pressure was set at 1.035 bars. Fig. 9 shows the step response of the plenum pressure applied at time 360 s (1.030 bar). The same figure shows the effect of adjusting the valve opening to 75% (at 710 s). In both cases the load split factor (λ) is automatically adjusted by the proposed LSO to minimize the total compression system energy consumption. The corresponding profile of λ in reaction to the changes mentioned above is shown in Fig. 10; The adaptive algorithm is seen running every 50 s (but λ will only change if there is a change in the operating conditions). A comparison of the total electrical energy consumption of the parallel operated compressors using the proposed LSO and using equal load sharing is depicted in Fig. 11; the results show a reduction of more than 4% in the total energy consumed by using the proposed LSO.

VII. HARDWARE IMPLEMENTATION

The proposed control structure and the adaptive load sharing algorithm presented in Fig. 2 are further validated experimentally in this section. The developed hardware setup is shown in Fig. 12. It consists mainly of two parallel compressors connected to a common plenum, and a throttle valve. Each compressor is controlled through a VFD, which receives its speed set-point through a Quanser q8-usb data acquisition card.

A. EXPERIMENTAL RESULTS

A manually tuned PID controller was implemented to control the desired pressure set-point at the common plenum (pressure tank) through varying the compressor speed set-points. Four different experimental conditions/operating points were tested with multiple operating conditions (different pressure set-points and valve openings) to validate the proposed control

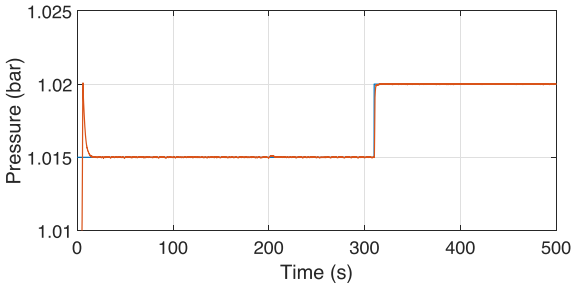

(a) Plenum pressure response to step change in pressure set-point at 310 s (experiment)

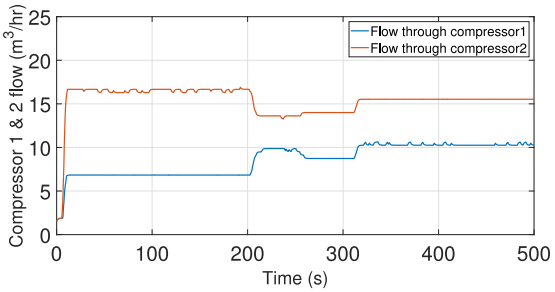

(b) First and second compressor volumetric flow rate (experiment)

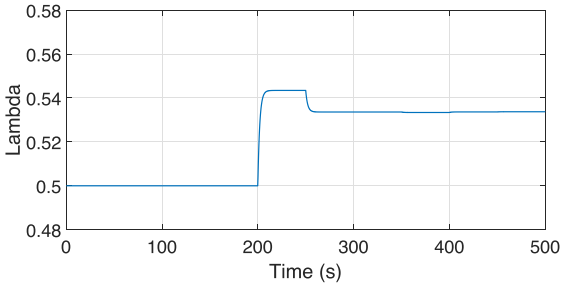

(c) Load split factor (λ) reaction to change of pressure set-point (experiment)

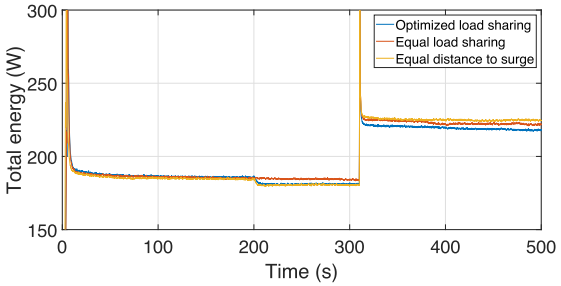

(d) Total energy consumption at equal distance to surge, equal load sharing, and optimal load sharing (experiment)

FIGURE 15. **Parallel compressor system energy consumption and dynamics response to changes in pressure set-point at 310 s (1.015 bar to 1.020 bar).**

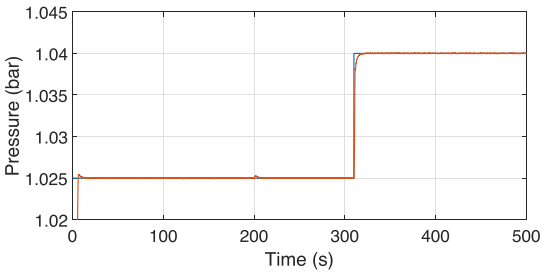

(a) Plenum pressure response to step change in pressure set-point at 310 s (experiment)

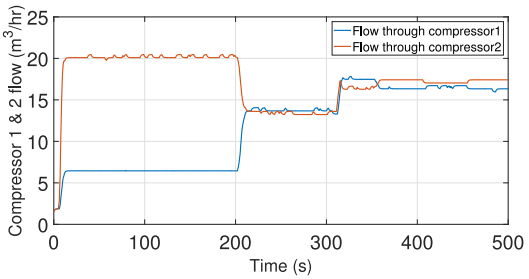

(b) First and second compressor volumetric flow rate (experiment)

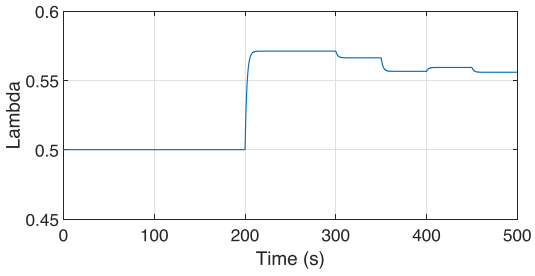

(c) Load split factor (λ) reaction to change of pressure set-point (experiment)

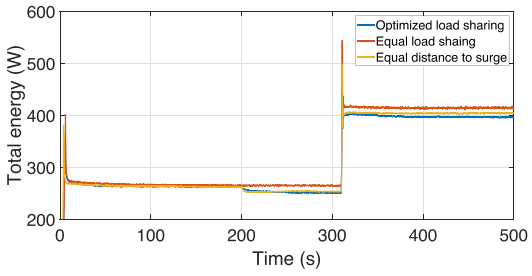

(d) Total energy consumption at equal distance to surge, equal load sharing, and optimal load sharing (experiment)

FIGURE 16. **Parallel compressor system energy consumption and dynamics response to changes in pressure set-point at 310 s (1.025 bar to 1.040 bar).**

structure and the adaptive LSO algorithm. The initial load split factor (λ) in all experimental results was 0.5 (equal load sharing between the two compressors). The proposed LSO algorithm starts running after 200 s to allow for the performance maps to be updated by the ERLSE algorithm. The LSO algorithm thereafter runs every 50 s. The updated compressor and performance maps of both compressors based on ERLSE algorithm (10) after running the experiment are shown in Fig. 13. The solid lines show the original performance maps derived experimentally at an early stage before connecting the overall setup, while the dashed lines are the updated performance maps that are used in the LSO algorithm. A slight

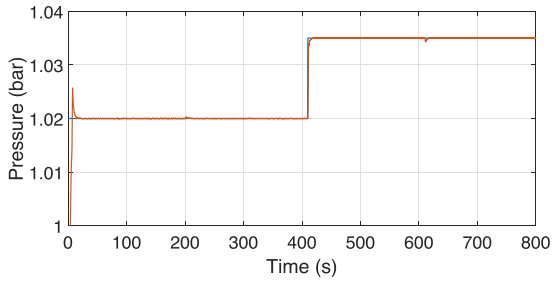

(a) Plenum pressure response to step changes in pressure set-point and valve opening at 410s and 610s, respectively (experiment)

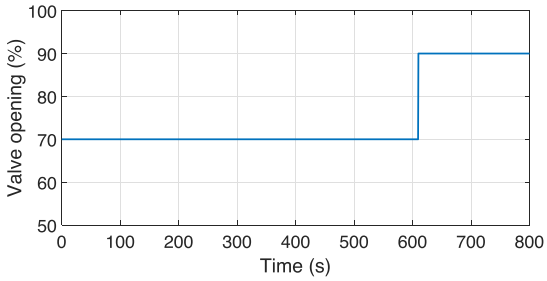

(b) Throttle valve opening (%)

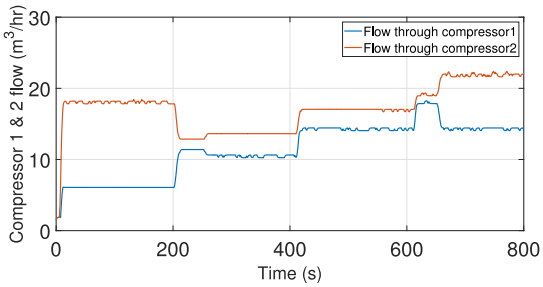

(c) First and second compressor volumetric flow rate (experiment)

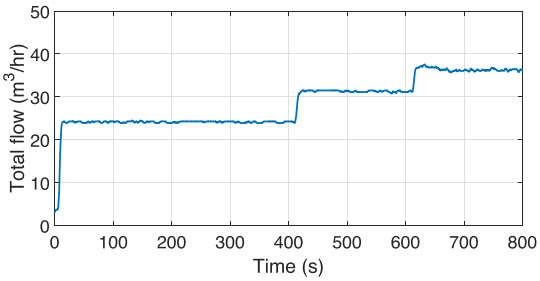

(d) Total throttle volumetric flow rate (experiment)

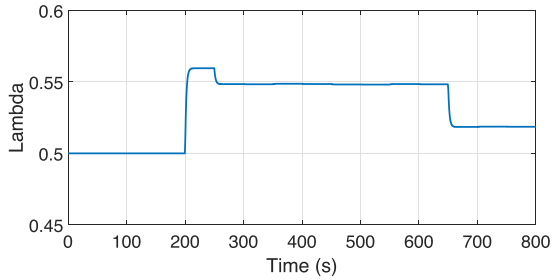

(e) Load split factor (λ) reaction to changes of pressure set-point and valve opening (experiment)

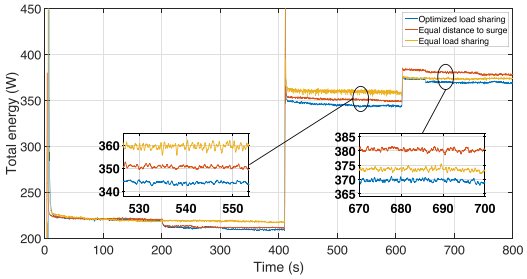

(f) Total energy consumption at equal distance to surge, equal load sharing, and optimal load sharing (experiment)

FIGURE 17. Parallel compressor system energy consumption and dynamics response to changes in pressure set-point at 410 s (1.020 bar to 1.035 bar) and valve opening at 610 s (70% to 90%).

change is observed due to the slight variation of the suction side air temperature. A higher change is expected on the long run due to the degradation and fouling of the compressors.

The first experimental conditions were the same as the ones in the simulation section. The initial valve opening was set to 80% and the tank pressure set-point was at 1.035 bar. Fig. 14(a) shows the plenum pressure response to a step change to 1.030 bar at 510 s and a change in valve opening to 70% at 710 s. The response of the adaptive controller LSO (change in load split factor) to these changes is shown in Fig. 14(c), and (b) depicts the effect of that on the flow through both compressors. The advantage of the proposed LSO algorithm over an equal load sharing scheme is clearly seen in Fig. 14(d) which shows the total energy consumption for either scheme subject to the same pressure set-point and valve opening changes. The hardware results (Fig. 14) show a high similarity to the simulation results (Figs. 9, 10, and 11) in terms of the adaptive controller reaction to changes in the pressure and valve set-points and the total energy consumption. The difference in the total energy consumption for the optimal load sharing is less than 1.5% and this is mainly due to the slow/small variation in the performance maps caused by fouling or slight temperature change of the air at the suction side as shown in Fig. 13. Figs. 15 and 16 depict the parallel compressor system energy consumption and dynamic response to changes in the pressure set-point at different operating conditions. The dynamic response of the pressure is shown in Figs. 15(a) and 16(a), while the dynamic response of the volumetric flow rate is shown in Figs. 15(b) and 16(b). Figs. 15(c) and 16(c) show how the load split factor is adjusted by the proposed adaptive LSO algorithm. Figs. 15(d) and 16(d) show the comparison of the total electric energy consumption resulting from the use of the proposed adaptive LSO algorithm, the equal distance to surge scheme, and the equal load sharing scheme. The superiority of the proposed adaptive LSO algorithm is clear. Fig. 17 provides another comparison of the three load sharing algorithms. The initial opening of the throttle valve was set to 80%. The plenum pressure set-point was initially at 1.020 bars. Fig. 17(a) shows the response of the pressure dynamics

to the set-point step change at 410 s to 1.035 bar and the decrease of the valve opening at 610 s to 70% (Fig. 17(b)). The proposed control structure provided a fast dynamic response to both changes in the pressure set-point and valve opening, without the need for an extra loop to decouple the two parallel compressors. The volumetric flow rate of the two compressors and the throttle valve are shown in Fig. 17(c) and (d), respectively. The response of the proposed adaptive LSO is seen in the load split factor (λ) profile shown in Fig. 17(e). The comparison of the total energy consumption using the three load sharing schemes is shown in Fig. 17(f). The results show a reduction of the total energy consumption in favor of the proposed LSO algorithm of up to more than 4% in comparison with the equal load sharing scheme and more than 2.5% in comparison with the equal distance to surge scheme. The adaptive algorithm reaction is depicted in the change of λ and a decrease of the total energy when the algorithm runs (every 50 s) depending on the current operating conditions.

VIII. CONCLUSION

This paper presents a novel load sharing adaptive control system for parallel operated compressors. It includes a structure with a single process controller and an optimization algorithm in the adaptation loop. The proposed control structure with a single process controller for multiple compressors promotes better stability and faster system dynamics with respect to set-point or disturbance changes. Moreover, it eliminates the need for having a loop decoupler between the compressors. Another contribution is the implementation of a recursive least square algorithm with exponential forgetting in real time to account for the gradual changes in the compressor and performance maps. In addition, an optimization algorithm is implemented within the adaptive control structure to minimize the total energy consumption. The designed LSO algorithm depends on the controller output, temperature and suction pressure of each compressor, and the derived compressor and performance maps. The designed system structure, on-line adaptive load sharing algorithm and the ERLSE are tested and verified using Matlab/Simulink simulations and further validated on a lab prototype. The proposed control structure showed a fast dynamic response to the changes in the required pressure set-point and valve opening. Moreover, the proposed algorithm improved the energy consumption by more than 4% compared to an equal load sharing scheme and more than 2.5% compared to the equal distance to surge scheme. The proposed control structure can be further improved by adding an automatic optimal tuning of PID parameters to improve the system's dynamic performance. Another research direction that can be explored is the design of MPC and comparing it with the proposed control structure.

REFERENCES

[1] P. Milosavljevic, A. G. Marchetti, A. Cortinovis, T. Faulwasser, M. Mercangöz, and D. Bonvin, "Real-time optimization of load sharing for gas compressors in the presence of uncertainty," *Appl. Energy*, vol. 272, 2020, Art. no. 114883. [Online]. Available: https://www.sciencedirect.com/science/article/pii/S0306261920303950

[2] R. Saidur, N. Rahim, and M. Hasanuzzaman, "A review on compressed-air energy use and energy savings," *Renewable Sustain. Energy Rev.*, vol. 14, no. 4, pp. 1135–1153, 2010. [Online]. Available: http://www.sciencedirect.com/science/article/pii/S1364032109002755

[3] D. P. Xenos et al., "Optimization of a network of compressors in parallel: Real time optimization (RTO) of compressors in chemical plants - an industrial case study," *Appl. Energy*, vol. 144, pp. 51–63, 2015.

[4] A. Cortinovis, M. Mercangöz, M. Zovadelli, D. Pareschi, A. D. Marco, and S. Bittanti, "Online performance tracking and load sharing optimization for parallel operation of gas compressors," *Comput. Chem. Eng.*, vol. 88, pp. 145–156, 2016.

[5] M. P. Boyce, "Centrifugal compressors: A basic guide," Tulsa, OK: PennWell Corporation, 2003. [Online]. Available: https://app.knovel.com/hotlink/toc/id:kpCCABG001/centrifugal-compressors/centrifugal-compressors

[6] H. Devold, *Oil and Gas Production Handbook. An Introduction to Oil and Gas Production, Transport, Refining and Petrochemical Industry*. Morrisville, NC, USA: Lulu.com, 2013, Art. no. 152.

[7] H. H. Nguyen, V. Uraikul, C. W. Chan, and P. Tontiwachwuthikul, "A comparison of automation techniques for optimization of compressor scheduling," *Adv. Eng. Softw.*, vol. 39, no. 3, pp. 178–188, 2008. [Online]. Available: https://doi.org/10.1016/j.advengsoft.2007.02.003

[8] S. Kumar and A. Cortinovis, "Load sharing optimization for parallel and serial compressor stations," in *Proc. IEEE Conf. Control Technol. Appl.*, 2017, pp. 499–504.

[9] R. Kurz and K. Brun, "Fouling mechanisms in axial compressors," *J. Eng. Gas Turbines Power*, vol. 134, no. 3, 2012, Art. no. 032401. [Online]. Available: https://doi.org/10.1115/1.4004403

[10] J. Petek and P. Hamilton, "Performance monitoring for gas turbines," *Orbit*, vol. 25, no. 1, pp. 64–74, 2005.

[11] F. Paparella, L. Dominguez, A. Cortinovis, M. Mercangöz, D. Pareschi, and S. Bittanti, "Load sharing optimization of parallel compressors," in *Proc. Eur. Control Conf.*, 2013, pp. 4059–4064.

[12] R. Kurz, M. Lubomirsky, and K. Brun, "Gas compressor station economic optimization," *Int. J. Rotating Machinery*, vol. 2012, 2012, Art. no. 715017.

[13] R. Tirnovan, S. Giurgea, A. Miraoui, and M. Cirrincione, "Surrogate modelling of compressor characteristics for fuel-cell applications," *Appl. Energy*, vol. 85, no. 5, pp. 394–403, 2008. [Online]. Available: http://www.sciencedirect.com/science/article/pii/S0306261907001158

[14] A. Demissie, W. Zhu, and C. T. Belachew, "A multi-objective optimization model for gas pipeline operations," *Comput. Chem. Eng.*, vol. 100, pp. 94–103, 2017. [Online]. Available: http://www.sciencedirect.com/science/article/pii/S009813541730073X

[15] A. Hawryluk, K. Botros, H. Golshan, and B. Huynh, "Multi-objective optimization of natural gas compression power train with genetic algorithms," in *Proc. Int. Pipeline Conf.*, 2010, pp. 421–435.

[16] M. Abbaspour, K. Chapman, and P. Krishnaswami, "Nonisothermal compressor station optimization," *ASME. J. Energy Resour. Technol*, vol. 127, pp. 131–141, 2005.

[17] M. Zagorowska, N. Thornhill, T. Haugen, and C. Skourup, "Load-sharing strategy taking account of compressor degradation," in *Proc. IEEE Conf. Control Technol. Appl.*, 2018, pp. 489–495.

[18] P. Milosavljevic, A. Cortinovis, R. Schneider, T. Faulwasser, M. Mercangöz, and D. Bonvin, "Optimal load sharing for serial compressors via modifier adaptation," in *Proc. Eur. Control Conf.*, 2018, pp. 2306–2311.

[19] M. Zagorowska, C. Skourup, and N. F. Thornhill, "Influence of compressor degradation on optimal operation of a compressor station," *Comput. Chem. Eng.*, vol. 143, 2020, Art. no. 107104. [Online]. Available: https://www.sciencedirect.com/science/article/pii/S0098135420305627

[20] P. Milosavljevic, R. Schneider, A. Cortinovis, T. Faulwasser, and D. Bonvin, "A distributed feasible-side convergent modifier-adaptation scheme for interconnected systems, with application to gas-compressor stations," *Comput. Chem. Eng.*, vol. 115, pp. 474–486, 2018. [Online]. Available: https://www.sciencedirect.com/science/article/pii/S0098135418304368

[21] X. Li, T. Cui, K. Huang, and X. Ma, "Optimization of load sharing for parallel compressors using a novel hybrid intelligent algorithm," *Energy Sci. Eng.*, vol. 9, no. 3, pp. 330–342, 2021. [Online]. Available: https://onlinelibrary.wiley.com/doi/abs/10.1002/ese3.821

[22] A. Cortinovis, H. Ferreau, D. Lewandowski, and M. Mercangöz, "Experimental evaluation of MPC-based anti-surge and process control for electric driven centrifugal gas compressors," *J. Proc. Control*, vol. 34, pp. 13–25, 2015.
[23] T. Bentaleb, A. Cacitti, S. De Franciscis, and A. Garulli, "Multivariable control for regulating high pressure centrifugal compressor with variable speed and igv," in *Proc. IEEE Conf. Control Appl.*, 2014, pp. 486–491.
[24] T. Bentaleb, A. Cacitti, S. De Franciscis, and A. Garulli, "Model predictive control for pressure regulation and surge prevention in centrifugal compressors," in *Proc. Eur. Control Conf.*, 2015, pp. 3346–3351.
[25] Y. Eldigair, F. Garelli, C. Kunusch, and C. Ocampo-Martinez, "Adaptive pi control with robust variable structure anti-windup strategy for systems with rate-limited actuators: Application to compression systems," *Control Eng. Pract.*, vol. 96, 2020, Art. no. 104282.
[26] R. S. Shehata, H. A. Abdullah, and F. F. G. Areed, "Fuzzy logic surge control in constant speed centrifugal compressors," in *Proc. Can. Conf. Elect. Comput. Eng.*, 2008, pp. 000653–000658.
[27] W. Jacobson et al., "Compressor loadsharing control and surge detection techniques," in *Proc. 45th Turbomachinery Symp. Turbomachinery Lab.*, 2016.
[28] N. Staroselsky, S. Mirsky, P. A. Reinke, P. M. Negley, and R. J. Sibthorp, "Load sharing method and apparatus for controlling a main gas parameter of a compressor station with multiple dynamic compressors," U.S. Patent 5 347 467, Sep. 13, 1994.
[29] A. Saxena and M. Ledizes, "Management and optimization of load sharing between multiple compressor trains for controlling a main process gas variable," U.S. Patent 6 602 057, Aug. 5, 2003.
[30] J. Dirks and P. Jansen, "Method and system for controlling a turbocompressor group," U.S. Patent 8 647 047, Feb. 11, 2014.
[31] A. J. Fisher, T. S. Smoot, and D. E. Kincer, "Method and apparatus for controlling a system of compressors to achieve load sharing," U.S. Patent 5 343 384, Aug. 30, 1994.
[32] P. Milosavljevic, A. Cortinovis, A. G. Marchetti, T. Faulwasser, M. Mercangöz, and D. Bonvin, "Optimal load sharing of parallel compressors via modifier adaptation," in *Proc. IEEE Conf. Control Appl.*, 2016, pp. 1488–1493.
[33] E. M. Greitzer, "Surge and rotating stall in axial flow compressors - part I: Theoretical compression system model," *J. Eng. Power*, vol. 98, no. 2, pp. 190–198, 1976.
[34] G. Torrisi, S. Grammatico, A. Cortinovis, M. Mercangöz, M. Morari, and R. S. Smith, "Model predictive approaches for active surge control in centrifugal compressors," *IEEE Trans. Control Syst. Technol.*, vol. 25, no. 6, pp. 1947–1960, Nov. 2017.
[35] J. T. Gravdahl, O. Egeland, and S. O. Vatland, "Drive torque actuation in active surge control of centrifugal compressors," *Automatica*, vol. 38, no. 11, pp. 1881–1893, 2002.
[36] J. T. Gravdahl and O. Egeland, "Centrifugal compressor surge and speed control," *IEEE Trans. Control Syst. Technol.*, vol. 7, no. 5, pp. 567–579, Sep. 1999.
[37] A. Cortinovis, D. Pareschi, M. Mercangoez, and T. Besselmann, "Model predictive anti-surge control of centrifugal compressors with variable-speed drives," in *Proc. 1st IFAC Workshop Autom. Control Offshore Oil Gas Prod.*, 2012, pp. 251–256.
[38] J. T. Gravdahl and O. Egeland, *Compressor Surge and Rotating Stall: Modeling and Control*. Berlin, Germany: Springer, 2012.
[39] O. Egeland and J. T. Gravdahl, "Modeling and simulation for automatic control," *Mar. Cybern. Trondheim*, vol. 76, 2002.
[40] M. Venturini, "Development and experimental validation of a compressor dynamic model," *J. Turbomachinery*, vol. 127, no. 3, pp. 599–608, 2004.
[41] S. Venant and Wantzel, "Mémoire et expériences sur Íécoulement de léair," *de Íécole polytechnique*, vol. 16, pp. 85–122, 1839.
[42] J. T. Gravdahl, A. Egeland, and S. O. Vatland, "Active surge control of centrifugal compressors using drive torque," in *Proc. 40th IEEE Conf. Decis. Control*, 2001, pp. 1286–1291.
[43] T. F. Øvervåg, "Centrifugal compressor load sharing with the use of MPC," Master's thesis, NTNU, Trondheim, Norway, 2013.
[44] L. Ljung, *System Identification: Theory for User*. Englewood Cliffs, NJ, USA: Prentice Hall, 1999.
[45] K. J. Åström and B. Wittenmark, *Adaptive Control*. North Chelmsford, Chelmsford, MA, USA: Courier Corporation, 2013.

AYMAN AL ZAWAIDEH (Member, IEEE) received the B.Sc. and M.Sc. degrees in electrical engineering from Khalifa University, Abu Dhabi, United Arab Emirates, in 2015 and 2017, respectively. He is currently a Research Associate with Khalifa University. His research interests include power converters, analysis and design of nonlinear systems, sliding mode control, and controller tuning.

KHALIFA AL HOSANI (Senior Member, IEEE) received the B.Sc. and M.Sc. degrees in electrical engineering from the University of Notre Dame, Notre Dame, IN, USA, in 2005 and 2007, respectively, and the Ph.D. degree in electrical and computer engineering from The Ohio State University, Columbus, OH, USA, in 2011. He is currently an Associate Professor with the Department of Electrical Engineering and Computer Science, Khalifa University, Abu Dhabi, United Arab Emirates. He is also an Engineering & Technology affiliate Member with the Mohammed bin Rashed Academy of Scientists. He is the Co-Founder of the Power Electronics and Advanced Sustainable Energy Center Laboratory, ADNOC Research and Innovation Center (now Power Electronics and Sustainable Energy (PEASE) Research Lab at Khalifa University) Abu Dhabi, United Arab Emirates. His research interests include a wide range of topics including nonlinear control, sliding mode control, control of power electronics, power systems stability and control, renewable energy systems modeling and control, smart grid, microgrid and distributed generation, and application of control theory to oil and gas applications.

IGOR BOIKO (Senior Member, IEEE) received the M.Sc., Ph.D., and D.Sc. (Habil.) degrees in electromechanical engineering and control system engineering. He is currently a Professor with the Department of Electrical Engineering and Computer Science, Khalifa University of Science and Technology, Abu Dhabi, United Arab Emirates. His research interests include discontinuous control, sliding mode control, power converter control, robotics, frequency-domain methods, and PID controller tuning. In particular, he developed such methods and concepts as the LPRS method, dynamic harmonic balance, phase deficit, fractal dynamics, and optimal non-parametric controller tuning. He has authored or coauthored four books and a number of journals and conference papers. He is a Member of the IEEE Technical Committee on Variable Structure Systems.

MOHAMMAD LUAI HAMMADIH received the B.Sc. and M.Sc. degrees in electrical engineering from Khalifa University, Abu Dhabi, United Arab Emirates. His research interests include nonlinear control, process control applications and sliding mode observers.